Cellular Signalling 59 (2019) 41–52

Contents lists available at ScienceDirect

Cellular Signalling

journal homepage: www.elsevier.com/locate/cellsig

Activation of PERK-eIF2α-ATF4 pathway contributes to diabetic hepatotoxicity: Attenuation of ER stress by Morin

Vivek Kumar Pandey[a,b], Alpana Mathur[a,c], Mohammad Fareed Khan[a,b], Poonam Kakkar[a,b,*]

[a] Herbal Research Laboratory, Food, Drug & Chemical Toxicology Group, CSIR-Indian Institute of Toxicology Research, Vishvigyan Bhavan 31, M.G Marg, Lucknow 226001, Uttar Pradesh, India
[b] Academy of Scientific and Innovative Research (AcSIR), CSIR-Indian Institute of Toxicology Research, Lucknow, India
[c] Babu Banarasi Das University, Lucknow, Uttar Pradesh, India

ARTICLE INFO

Keywords:
Apoptosis
Diabetes
ER stress
Hyperglycemia
Morin

ABSTRACT

Hyperglycemia associated ER stress has been found as a critical contributor in the pathogenesis of type 2 diabetes mellitus. However, reports regarding molecular mechanisms involved are limited. This study was aimed to identify the role of ER stress in regulating hepatic glucose metabolism and its link with oxidative stress. Further, this study explores the novel role of Morin, a flavonol, in modulating ER stress in STZ/nicotinamide induced type 2 diabetic male Wistar rats. Results demonstrate that hyperglycemia induced ER stress in rats and significantly lowered the expression of glucose transporter proteins resulting in impaired glucose metabolism during diabetes. Morin was found to downregulate PERK-eIF2α-ATF4 pathway by interacting with PERK protein as confirmed through pull-down assay. Additionally, Morin maintained the reducing environment in ER and enhanced PDI activity compared to diabetic rats. Morin prevented cell death by suppressing the expression of PERK dependent pro-apoptotic proteins including ATF4 and CHOP. Findings from this study affirm the role of ER stress in hyperglycemia induced gluco-metabolic aberrations and liver injury as confirmed by ISRIB, a standard chemical ER stress inhibitor. Notably, Morin promoted deactivation of UPR sensors and upregulated PDI activity endorsing its anti-ER stress potential which may allow the development of new therapeutic avenues to target hyperglycemic hepatotoxicity.

1. Introduction

Impaired insulin production and/or action causes a pronounced increase in blood glucose levels (hyperglycemia) which is associated with organopathies including retinopathy, nephropathy, neuropathy and cardiovascular disorders [1–4]. Liver plays a cardinal role in the glucose homeostasis as the majority of genes involved in the glucose metabolism and storage reside in hepatocytes [5]. Insulin resistant conditions amplify hepatic glucose output and subsequent non-suppressible hyperglycemia which leads to diabetic hepatopathy [6]. Hyperglycemia further induces oxidative stress causing subcellular and macromolecular damages, of which ER stress has been reported as a contributing factor during several diabetic etiologies [7,8]. Proteins being most abundant amongst other cellular macromolecules, are susceptible to oxidation through ROS [9] and creates an extra load on ER for protein synthesis, folding and trafficking. ER resident proteins/chaperones also undergo destruction due to increased organellar oxidative stress leading to obstructive accumulation of misfolded proteins in ER [10]. Thus, disturbed ER homeostasis activates UPR (unfolded protein response) sensor proteins, *i.e.* PERK (protein kinase RNA like endoplasmic reticulum kinase), IRE1α (inositol requiring enzyme 1) and ATF6 (activating transcription factor 6) to restore the equilibrium [11–15]. Activated PERK phosphorylates eIF2α (eukaryotic initiation factor 2α) at Ser51 which prevents the formation of eIF2-GTP-Met-$tRNA_i^{Met}$ ternary complex thereby inhibiting global protein synthesis by constraining to the failure of translation initiation. Hence, activated PERK helps in lowering the overall protein load in ER [16]. Concurrently, phosphorylation of eIF2α at ser51 promotes translation of selective mRNAs that contain internal ribosomal entry site (IRES) including ATF4 (activating transcription factor 4) and CHOP (CEBP homologous protein) proteins [16,17]. Initially, ATF4 and CHOP promote autophagy by enhancing the expression of p62, Atg10 (autophagy related 10), Atg5 and Atg7 to degrade the protein cargos while sustained proteotoxicity promotes ATF4/CHOP mediated cell death

* Corresponding author at: Herbal Research Laboratory, CSIR-Indian Institute of Toxicology Research, Vishvigyan Bhawan 31, M.G Marg, Lucknow 226001, Uttar Pradesh, India.
E-mail address: pkakkar@iitr.res.in (P. Kakkar).

https://doi.org/10.1016/j.cellsig.2019.03.008
Received 24 December 2018; Received in revised form 22 February 2019; Accepted 6 March 2019
Available online 12 March 2019
0898-6568/

[17–19]. Involvement of UPR pathways in regulating pancreatic β-cell function is well documented however, studies explicating UPR signaling in diabetic hepatopathy are lacking. The present study for the first time elucidates evidence for the direct involvement of ER stress in hepatic physiology, glucose uptake, oxidative stress and liver damage under hyperglycemic milieu. We validated the intervention of ER stress by using its chemical inhibitor, ISRIB [integrated stress response inhibitor (trans-N, N′-(Cyclohexane-1,4-diyl)bis (2-(4-chlorophenoxy) acetamide)], in streptozotocin (STZ)/ nicotinamide induced type 2 diabetic male Wistar rats. Towards safer and effective therapy, phytochemicals have shown promising results in the management of diabetes. Morin (2′,3,4′,5,7-pentahydroxyflavone), a flavonol found in guava, orange, mulberry and in other plants of *Myrtaceae* family, is well known for its anti-hyperglycemic, anti-oxidative and anti-inflammatory properties [20]. Importantly, Morin also inhibits PTP1B (protein tyrosine phosphatases 1B) and exerts an insulin-mimetic effect in HepG2 cells [21], suggestive of its potency in diabetes management. Earlier studies from our lab have demonstrated that Morin prevented liver and kidney injury by attenuating drug/high glucose induced oxidative stress [20,22–24]. Based on these multiple evidence, we compared the effects of ISRIB with Morin. Further, we employed Morin to identify its role in ER stress management. This study also focuses on the impact of Morin in attenuating hyperglycemia mediated proteotoxic apoptosis by modulating PERK-p-eIF2α-ATF4 axis during high glucose induced ER stress. ISRIB was also used as a positive control of ER stress inhibitor to compare the anti-ER stress efficacy of Morin. This study therefore explores the underlying mechanism behind deleterious effects in the progression of chronic liver disease during T2DM (Type 2 diabetes mellitus) and reveals the novel molecular interaction of Morin for its anti-diabetic potential *via* inhibition of ER stress induced proteotoxic apoptosis.

2. Materials and methods

2.1. Materials

Antibodies including PERK (sc-13073), eIF2α (sc-11386), Caspase-3 (sc-7148), β-actin (sc47778), Bax (sc-493), Bcl2 (sc-492), AIF (sc-9417), EndoG (sc-26923), Cytochrome c (sc-8385), c-PARP (sc-23461), GLUT2 (sc-9117), CD36 (sc-9154), ICAM1 (sc-1511), Nrf2 (sc-13032), NQO1 (sc-16463), HO1 (sc-10789), SOD2 (sc-18503), HRP tagged anti-goat (sc-2354), Phosphocruz agarose beads (sc-24957) and Protein A/G Plus sepharose beads (sc-2003) were purchased from Santa Cruz Biotechnology (Santa cruz, CA). p-eIF2α (3597), BiP (3183), CHOP (2895), ATF4 (11815), PDI (3501P), Calpain1 (2556), Bim (2819S), Histone3 (4499S), Cox IV (11967S), TNFα (3707S), HRP tagged anti-mouse (7076S) antibody and anti-mouse/anti-rabbit FITC conjugated secondary antibodies (4408S/4413S) were procured from Cell Signaling Technology (CST, Danvers MA 01932). IRE-1α (ab37073), ATF-6 (ab203119), XBP-1 (ab198999), and GLUT4 (ab654) were purchased from Abcam, Cambridge MA, USA. Streptozotocin (85882), Nicotinamide (N3376), Morin (M4008), Glucose (G8270) ISRIB (SML0843), Hoechst 33258, Nytrotyrosine (N0409), HRP tagged anti-rabbit (A0545) antibody and all other chemicals were procured from Sigma (St Louis, MO, USA).

2.2. Animals

Animal studies were conducted in accordance with the international guidelines and protocols approved by the Institutional Animal Ethics Committee of CSIR-IITR vide approval document number IITR/IAEC/01/2016. Male Wistar rats [(*Rattus norvegicus),* 180–200 g (~4 weeks)] were procured from IITR animal facility and housed in experimental rooms with controlled temperature (22 ± 2 °C), humidity (60–70%) and regular light cycles (12 h each). Rats were maintained on a standard pellet diet (Altromin International, Germany) and water *ad libitum*.

2.3. Induction of diabetes in rats

Type 2 diabetes was induced in rats by single intra-peritoneal injection of streptozotocin (60 mg/Kg bwt.). Prior to STZ treatment, rats were injected with nicotinamide (120 mg/Kg bwt.) in normal saline while control rats were received only normal saline [25]. Nicotinamide prevents STZ induced DNA damage by inhibiting PARP1 activity and enhancing NAD^+ levels in cells. STZ-NA also induces mild diabetes which remains stable for a long time. After 3 days of injection, rats, whose random glucose levels were higher than 250 mg/dL served as diabetic and were selected for further experiments. STZ-NA induced diabetic rats are useful to study molecular aspects of diabetic complications and assessment of the anti-diabetic potential of natural compounds as it partially damages pancreatic β-cells [26,27]. A group of diabetic rats was treated with Morin (30 mg/Kg bwt./day) by oral gavage while ISRIB (0.125 mg/Kg/day) was given intra-peritoneally to another group of diabetic rats (n = 5). Moreover, a control group was also supplemented with Morin (30 mg/Kg bwt./day) to check if any adverse effect is caused by Morin itself.

2.4. Insulin tolerance test (ITT)

Overnight fasted rats were used to stabilize dietary glucose and insulin levels as described previously by Kubota et al., 2000 [28]. Briefly, ~10 μlL tail vein blood was collected to ascertain fasting glucose levels. Rats then received 1.5 U kKg^{-1} of insulin by intraperitoneal injection. Sample tail tip blood glucose levels were assessed by glucometer at 0, 15, 30 and 45 min.

2.5. Oral glucose tolerance test (OGTT)

OGTT was performed by administration of glucose at (2 g/Kg bwt.) by oral gavage. Blood samples (~ 10 μL/sample from the tail vein) were collected immediately before administration (0 min) and at 30, 60, 90 and 120 min after oral glucose treatment for measurement of circulating blood glucose levels [29].

2.6. Protein disulfide isomerase (PDI) assay

PDI is a major ER resident protein responsible for the correct disulfide bond formation of the proteins and plays a critical role in the ER and cellular redox homeostasis [30]. PDI activity was assessed using insulin turbidity method as described by Townsend et al., 2009 and Bernardoni et al., 2013 with slight modifications [31,32]. Briefly, 500 μg of each sample was incubated with a solution of 0.1 M KH_2PO_4 (pH 7.0) buffer and 2 mM EDTA followed by addition of 10 mg/mL of Insulin and 1 mM GSH solution, for 30 min at 37°C. Increasing turbidity of reduced insulin was measured at λ = 630 nm for 1 h at 5 min interval. Results are expressed as total insulin reduction (turbidity)/mg protein.

2.7. Subcellular fractionation

2.7.1. Nuclear, mitochondrial and cytosolic fractionation

Nuclear, mitochondrial and cytosolic fractions were obtained as described by Dimauro et al., 2012 [33]. Briefly, 100 mg liver tissue was minced and homogenized using homogenizer (IKA labortechnike, Janke & Kankle, Germany) and thereafter suspended in ice cold 5 mL of STM buffer [250 mM sucrose, 50 mM TrisHCl (pH 7.4), 5 mM $MgCl_2$] along with protease and phosphatase inhibitor cocktails. The homogenate was allowed to rest on ice for 30 min, vortexed twice for 15 s and then centrifuged at 800 × *g* for 15 min. The supernatant was then used for subsequent isolation of mitochondrial and cytosolic fractions while the pellet was re-suspended in STM buffer followed by sonication in NET buffer (20 mM HEPES pH 7.9, 1.5 mM $MgCl_2$, 0.5 M NaCl, 0.2 mM EDTA, 20% glycerol, 1% triton-X-100). Further, supernatant for

isolation of cytosolic and mitochondrial fractions was centrifuged at 11,000 ×*g* for 10 min. The pellet was re-suspended in SOL buffer (50 mM Tris HCl pH 6.8, 1 mM EDTA, 0.5% Triton-X-100) and after sonication it served as mitochondrial fraction while the supernatant served as cytosol after precipitation with 100% acetone and subsequent suspension in STM buffer.

2.7.2. Microsomal fractionation

Microsomal fractions were isolated according to Cox and Emili, 2006 [34]. Briefly, liver tissues were homogenized in 250 mM STMDPS buffer (250 mM sucrose, 50 mM Tris-HCl, pH 7.4; 5 mM $MgCl_2$ 1 mM DTT, 25 mg mL^{-1} Spermine, 25 mg mL^{-1} Spermidine and 1 mM PMSF). Homogenate was ultra-centrifuged at 100,000 ×*g* for 1 h, the pellets obtained were used for microsome isolation. The pellet were re-suspended in membrane extraction buffer [20 mM Tris-HCl (pH 7.8), 0.4 M NaCl, 15% glycerol, 1 mM DTT, 1 mM PMSF and 1.5% Triton-X-100] and centrifuged at 9000 ×*g* for 30 min. The supernatant was labelled as the microsomal fraction.

2.8. Co-immunoprecipitation

Interaction of PERK and BiP proteins as well as levels of phospho-PERK were assessed by co-immunoprecipitation as described previously by Cottrell et al., 2006 [35]. Approximately, 500 μg of protein from liver tissue lysate prepared in non-denaturing NP-40 lysis buffer (20 mM HEPES pH 7.4, 1% NP-40, 1 mM DTT and inhibitor cocktails) was incubated on tube rotator with anti-PERK antibody for 2 h at 4̊ C, after which, 20 μL of Protein A/G PLUS sepharose beads were added and rotated on tube rotator overnight at 4̊°C. For phosphorylated PERK, we incubated 500 μg of protein with phosphocruz-agarose beads in NP-40 medium. The beads were rinsed thrice with the lysis buffer and boiled in 2× SDS loading dye. The protein samples were run across 10% SDS-PAGE and then transferred onto PVDF membrane. Primary antibody against BiP protein was applied to the membrane at a dilution of 1:1000. Blots were washed thrice with TBST (10 min) before their incubation with 2° antibodies (1:2000) for 3 h on a shaker. Blots were then washed again thrice with TBST (10 min) and visualized using Immobilon western chemiluminescent horseradish peroxidase substrate kit (Millipore Corporation, Billerica, MA, USA) on Amersham Imager 600 detection system (GE Healthcare,UK) and the protein levels were analyzed by ImageJ1.44p software (National Institute of Health, Bethesda, MD,USA).

2.9. Pull down assay

Activation of sepharose beads and its coupling with Morin was performed according to the method described by Rizvi et al., 2015 [22]. Briefly, 300 mg of CNBr activated sepharose 4B beads were suspended in 10 mL of 1 M HCl. The swollen beads were washed 10 times (15 min/washing) with 1 M HCl and at last with coupling buffer (0.1 M $NaHCO_3$ pH 8.3, 0.5 M NaCl). The medium was further divided into two, one as blank and the other for morin coupling. 2 mg Morin dissolved in 100 μL of DMSO was added to the medium containing beads and a final volume of 1.5 mL was achieved with the addition of coupling buffer. To the blank, 100 μL DMSO was added to the beads and coupling buffer to make 1.5 mL volume. The suspension was rotated end to end overnight at 4 °C followed by washing and blocking of the Morin conjugated and blank beads.

The beads were washed twice with reaction buffer (50 mM Tris pH 7.5, 5 mM EDTA, 150 mM NaCl, 1 mM DTT, 0.01% NP-40, 2 mg/mL BSA, 0.02 mM PMSF and protease inhibitor cocktail). 100 μg protein of hepatic lysate was incubated overnight on the tube rotator with 50 μL of conjugated sepharose beads and blank beads separately in reaction buffer at 4̊°C. The pull-down protein was washed thrice with reaction buffer and samples were boiled with 2× SDS loading dye. 10% SDS-PAGE was used to separate the proteins followed by their transfer on PVDF membrane and probing with UPR sensor proteins separately.

2.10. Statistical analysis

Results are presented as mean ± SE. Statistical comparisons between means of different groups were conducted by one-way Analysis of Variance (ANOVA). Differences were considered statistically significant when $p < 0.05$.

Rest of the methods are provided in Supplementary material.

3. Results

3.1. Hyperglycemia induces endoplasmic reticulum stress in Wistar rats

Imbalance in redox homeostasis is a cardinal feature in the early initiation of ER dysfunction, characterized by the impairment in ER resident protein folding enzymes. Thus, to assess whether hyperglycemia evokes dysfunction in ER, we determined the activity of PDI (protein disulfide isomerase), an important protein folding enzyme in liver tissue lysates using insulin reduction assay. To validate if the changes were entirely due to ER stress, we employed an ER stress inhibitor, ISRIB at a concentration of 0.125 mg/Kg bwt. per day (Fig. 1A). Results demonstrate that PDI activity was significantly reduced (0.72 fold; $p < 0.05$) during diabetes (Fig. 1B) while ISRIB treatment enhanced PDI activity by 3.17 fold ($p < 0.05$) compared to diabetic rats suggesting that hyperglycemia advances ER stress in rat liver (Fig. 1B). Since thiols play a major role in the protein folding activity of PDI, we measured total thiols and GSH/GSSG ratio in ER lumen to correlate the cause for decreased PDI activity in diabetic rats. Results demonstrate that total thiols and GSH/GSSG ratio reduced significantly in the microsomal fractions of diabetic rats compared to control reflecting shortfall of reducing equivalents in ER (Fig. 1C, D). ISRIB treatment efficiently enhanced total thiol content (1.30 fold) and GSH/GSSG ratio (2.28 fold); $p < 0.05$ compared to diabetic rats, supporting the fact that hyperglycemia mediated lowering of reducing equivalents diminished PDI activity in diabetic liver (Fig. 1C, D).

Next, the expression of ER specific marker proteins was measured to identify the role of hyperglycemia in inducing ER stress. Data demonstrate that hyperglycemia activated PERK, a major UPR sensor protein, by significantly enhancing its phosphorylation in diabetic rats (1.79 fold, $p < 0.05$) compared to control (Fig. 1E). Other UPR sensor molecules were also up-regulated including IRE-1 (1.15 fold) and ATF6 (1.56 fold); $p < 0.05$ implicating activation of hyperglycemia induced ER stress response (Fig. 1F). Protein level of PDI was also reduced in diabetic rats (Fig. 1F) which was in confirmation with its reduced enzymatic activity (Fig. 1B) validating the impaired chaperone activity during diabetes. Further, the downstream factors of PERK signaling pathway were tracked where immunoblotting studies showed that PERK responsive proteins including p-eIF2α (1.58 fold), ATF4 (1.54 fold) and CHOP (3.94 fold); $p < 0.05$ were enhanced significantly in diabetic rat liver compared to control suggesting activation of proteotoxic apoptosis cascade (Fig. 1G, H). Selective ER stress inhibition (ISRIB) significantly lowered the expression of downstream targets of PERK *i.e.* p-eIF2α, ATF4 and CHOP compared to diabetic rats confirming activation of PERK signaling during T2D (Fig. 1G, H).

3.2. Hyperglycemia induced ER stress is integrated with oxidative stress: amelioration by Morin

Generation of excessive reactive oxygen species (ROS) is the major contributing factor in the progression of diabetic etiologies however, its correlation with oxidative stress is poorly understood in context of T2D. Therefore, we examined the redox status and assessed its modulation upon ER stress inhibition. In addition, we checked the effects of a flavonol, Morin (Fig. 2A) and compared it with the response generated by ER stress inhibitor, ISRIB. Results demonstrate that hyperglycemia

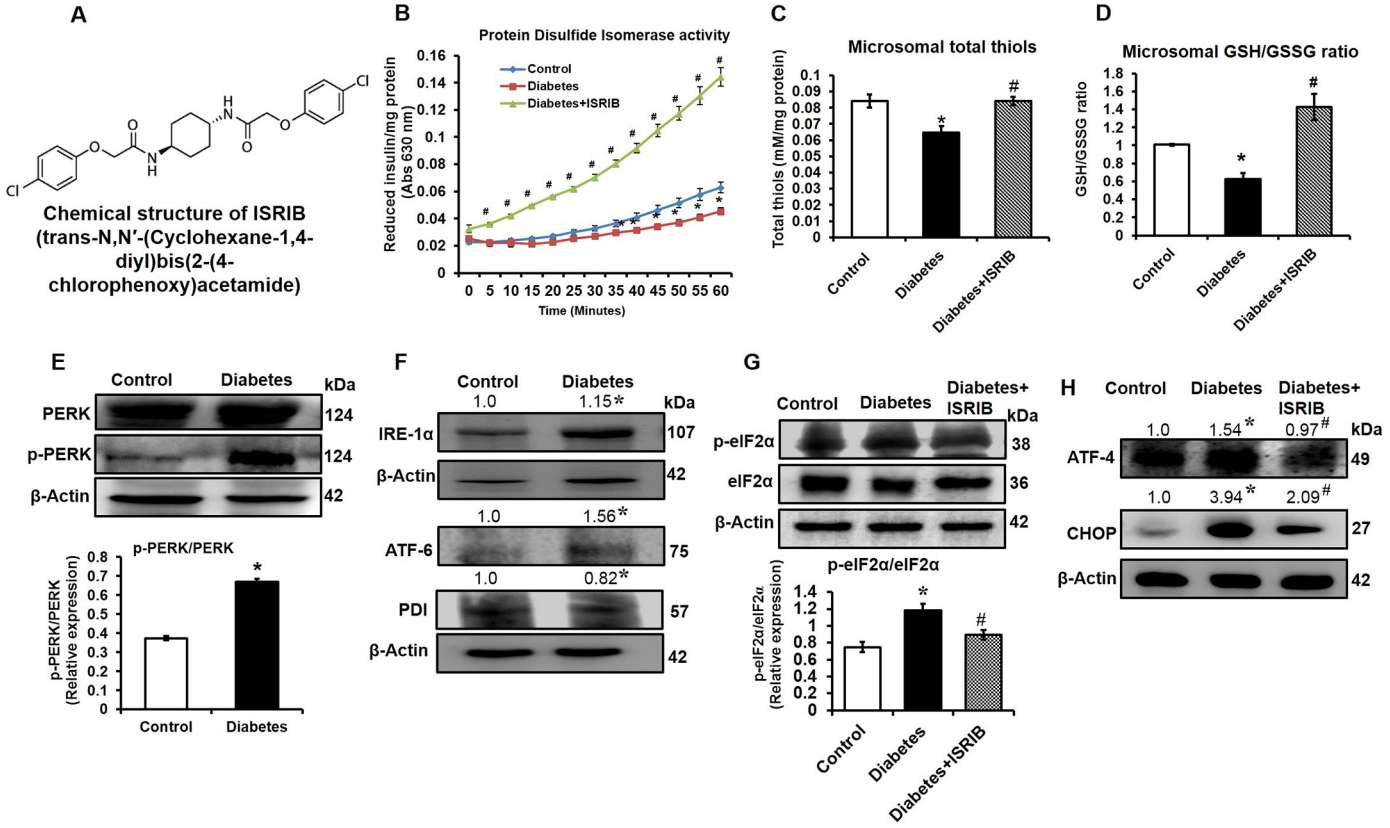

Fig. 1. Hyperglycemia induces endoplasmic reticulum stress in diabetic rats. Effect of high glucose on the ER homeostasis and stress markers was assessed in STZ/Nicotinamide induced T2D rats. (A) Chemical structure of the standard ER stress inhibitor, ISRIB (integrated stress response inhibitor), used for demonstrating the involvement of ER stress in hyperglycemic hepatotoxicity. (B) Protein disulfide isomerase (PDI) activity assessed using insulin reduction method. The graph represents absorbance of reduced insulin per mg protein. (C) Total thiol content in microsomal fractions expressed as mM total thiol levels per mg protein. (D) GSH/GSSG ratio in microsomal fractions of control and treated rat liver. (E) Protein levels of PERK and p-PERK were measured by immunoblotting, the bar graph shows relative densitometry of p-PERK normalized with PERK protein. Immunoblots of (F) IRE-1α, ATF-6, and PDI (G) p-eIF2α and eIF2α, the bar graph represents densitometric ratio of p-eIF2α/eIF2α. (H) Western blots of ATF4 and CHOP proteins. β-actin served as loading control for all western blots. Data are expressed as mean ± SE/SD. *p < 0.05 vs control and #p < 0.05 *vs* diabetic rats.

significantly enhanced oxidative stress as evident by increased TBARS levels (2.71 fold, $p < 0.05$) compared to control rats (Fig. 2B) indicating peroxidation of lipids. Interestingly, ER stress inhibition with ISRIB as well as Morin treatment lowered lipid peroxidation compared to diabetic rats (Fig. 2B). Further, total thiol levels were increased with ISRIB (2.28 fold) and Morin (1.33 fold) ($p < 0.05$) treatments compared to diabetic rats (Fig. 2B). Oxidative stress provoked protein carbonylation (9.41 fold, $p < 0.05$) during diabetes while ISRIB and Morin reduced it significantly (Fig. 2C) asserting that ER stress inhibition prevents excessive free radical damage.

Enhanced oxidative stress during diabetes resulted in the significant loss of antioxidant enzyme activities including catalase (0.49 fold), glutathione S-transferase (0.59 fold), thioredoxin reductase (0.56 fold) and glutathione peroxidase (0.28 fold); $p < 0.05$ compared to control (Fig. 2D). Contrarily, ER stress inhibition (ISRIB) and Morin treatment attenuated oxidative stress as evident through increased antioxidant enzyme activities suggesting an interlink between ER stress and oxidative stress. Moreover, Morin as well as ISRIB treatment also fortified cellular GSH and SOD2 levels compared to diabetic rats (Fig. 2E, F). Furthermore, expression of the critical redox sensitive transcription factor, Nrf2 and its downstream targets (NQO1 and HO1) were significantly up-regulated with ISRIB and Morin treatments compared to diabetic rats (Fig. 2G). Increased nuclear translocation of Nrf2 was observed through immunohistochemistry in ISRIB and Morin treated rats explicating their anti-oxidative response during T2D (Fig. 2H). Overall, results suggest that inhibition of ER stress by ISRIB reduced oxidative stress similar to Morin confirming that hyperglycemia induced ER stress and oxidative stress are interlinked ensuing diabetic complications.

3.3. ER stress inhibition improves hepatic metabolism in diabetic rats

Upon validation of ER stress induction in the diabetic liver, its impact on liver glucose metabolism was further ascertained. After 30 days of diabetes induction, diabetic rats showed significantly elevated random blood glucose levels (5.37 fold; $p < 0.05$) compared to control (Fig. 3A) while ISRIB treated rats exhibited reduced blood glucose levels by 53% ($p < 0.05$) compared to diabetic rats, suggesting that suppression of ER stress has a direct role in regulating blood glucose levels. Furthermore, Morin treatment significantly decreased blood glucose levels by 69.42% ($p < 0.05$) compared to diabetic rats showing its anti-hyperglycemic capacity (Fig. 3A). In addition, oral glucose tolerance test (OGTT) revealed that ISRIB treatment enhanced blood glucose clearance compared to diabetic rats. Thus, these results indicate the effect of ER stress on glucose homeostasis (Fig. 3B). Morin treated rats also tolerated glucose challenge and lowered the glucose load compared to diabetic rats implicating its strong anti-diabetic potential (Fig. 3B).

Hyperglycemia is associated with lack of insulin sensitivity (insulin resistance) thus, we estimated insulin tolerance capacity through ITT assay in rats where an insulin shot of 1.5 U/Kg bwt. lowered the blood glucose levels in Morin treated rats (0.48 fold; $p < 0.05$) compared to diabetic rats (Fig. 3C). Interestingly, inhibition of ER stress by ISRIB also improved the insulin action as evident by lowered blood glucose

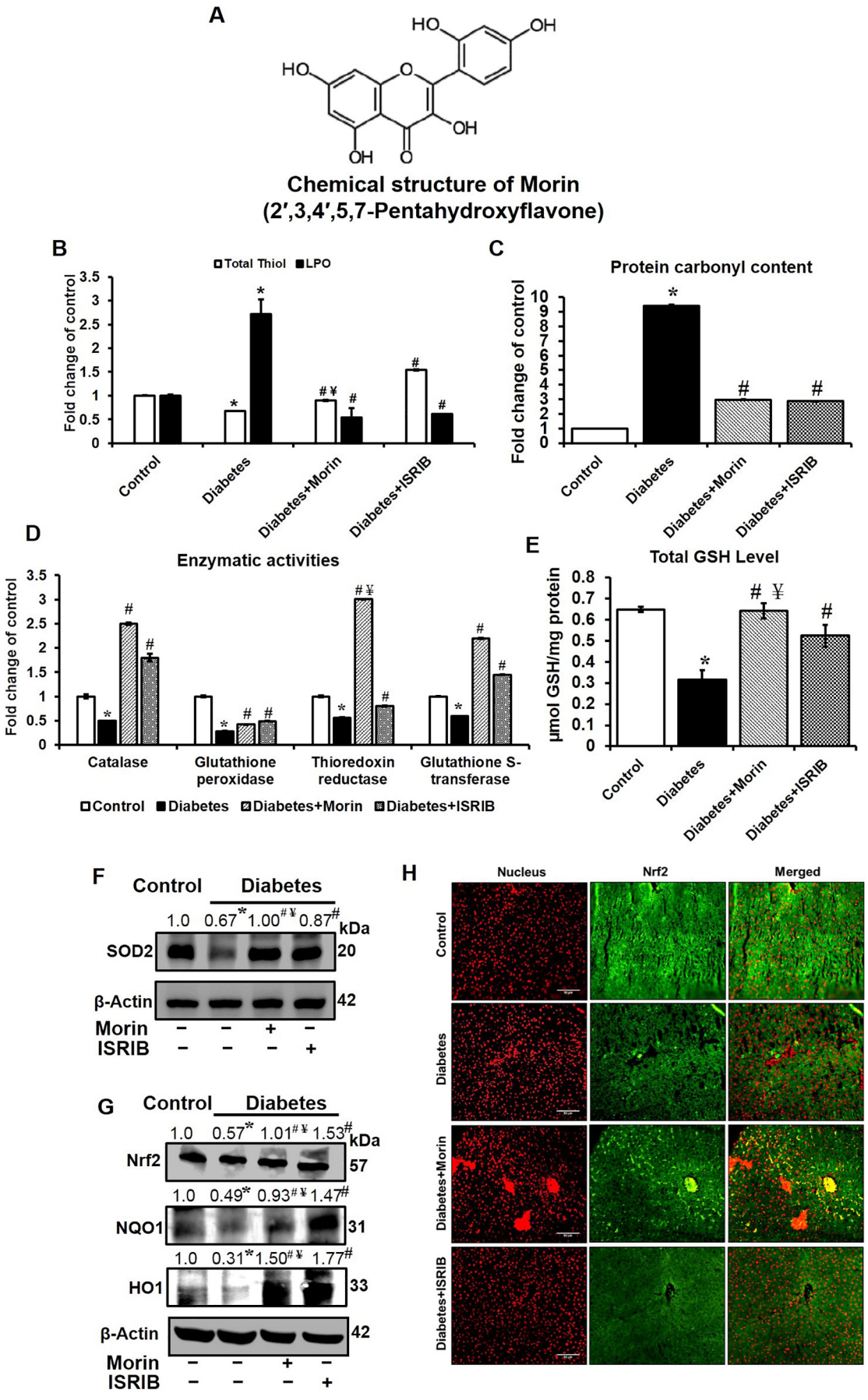

(caption on next page)

Fig. 2. ER stress inhibition lowers oxidative stress by concomitantly enhancing anti-oxidative potential in diabetic rat liver. (A) Chemical structure of the flavonol, Morin. Role of ER stress in oxidative damage was measured by evaluating (B) Total thiols and lipid peroxidation (LPO) levels in liver tissue lysate, represented as fold change of control. (C) The graph indicates protein carbonyl content in rat liver tissue lysate, data presented as fold change of control. Antioxidant enzyme activities of (D) Catalase, Glutathione Peroxidase (GPx), Thioredoxin Reductase (TxR) and Glutathione S-transferase (GST) were determined in total liver tissue lysates, and presented as fold change of control. (E) Total GSH content was estimated in lysates from treated rats, data presented as μmol of GSH/mg protein. (F) Immunoblot of SOD2 and (G) Nrf2, NQO-1 and HO-1 proteins. β-Actin served as loading control. (H) Immunohistochemical staining of Nrf2 and propidium iodide (PI; for nuclear stain) on 5 μm liver tissue sections (magnification 20×, scale bar; 50 μm). Data are expressed as mean ± SE. *p < 0.05 *vs* control, #p < 0.05 *vs* diabetic rats and ¥p < 0.05 *vs* ISRIB treated diabetic rats.

levels (Fig. 3C).

Importantly, a set of control rats treated with only Morin (30 mg/Kg bwt. per day) did not show any adverse effect on hepatic glucose metabolism as analyzed through blood glucose levels and glucose tolerance assays (Fig. 3A–C). Results obtained from Morin only treated rats (Control + Morin) were similar to that of normal rats (control rats) thereby excluding any possibility for metabolic aberration or toxicity caused by Morin (Fig. 3A–C).

Elevated blood glucose level promotes transportation of glucose transporter proteins for effective glucose uptake in the liver however, disturbed metabolic homeostasis during diabetes causes impaired glucose import. Thus, we inspected the expression of major glucose transporters, GLUT2 (insulin independent) and GLUT4 (insulin dependent) in the liver tissue lysate of treated rats. Immunoblotting data revealed lowered expression of GLUT2 and GLUT4 proteins in diabetic rats (Fig. 3D). A significant increase was observed in the protein expression of glucose transporters upon ER stress inhibition by ISRIB compared to diabetic rats, demonstrating a clear intervention of ER stress in glucose absorption (Fig. 3D). Importantly, Morin treatment enhanced the expression of GLUT2 and GLUT4 proteins demonstrating its glucose lowering potential (Fig. 3D). Therefore, it is evident from the results that hyperglycemia mediated ER stress manifests metabolic disturbances in liver which is prevented by Morin.

3.4. Morin attenuates ER stress mediated diabetic liver injury

Type 2 diabetes is reported to be associated with liver diseases [5,6]. In this study, histopathological examination of liver tissues by H&E staining showed hepatic congestion of central veins and distorted sinusoids in diabetic rats, while ER stress inhibition by ISRIB as well as Morin treatment prevented liver damage as evident by the intact central veins and sinusoids (Fig. 4A). Further, PAS staining was performed to examine glycogen deposition in liver tissues. Enhanced lymphoid infiltration and short septa formation were observed in diabetic liver (Fig. 4B). Contrarily, ISRIB and Morin treatments significantly prevented hepatic tissue damage and inflammation (Fig. 4A, B). Whereas, control rats supplemented with only Morin also showed normal morphology implicating no hepatocellular injury or inflammation due to Morin itself (Fig. 4A, B).

Liver enlargement, a feature of the liver disease, was increased in diabetic rats as evident through enhanced liver weight/body weight ratio (Fig. 4C). However, ISRIB as well as Morin treatment reduced liver weight/body weight ratio compared to diabetic rats (Fig. 4C). Morin treated rats also showed prevention in excessive body weight loss as observed in diabetic rats. However, ISRIB treatment could not prevent weight loss significantly (Fig. 4D). Body weight and liver/body weight ratio of only Morin treated rats were similar to that of control (normal rats) indicating no adverse effect of Morin itself on rat physiology

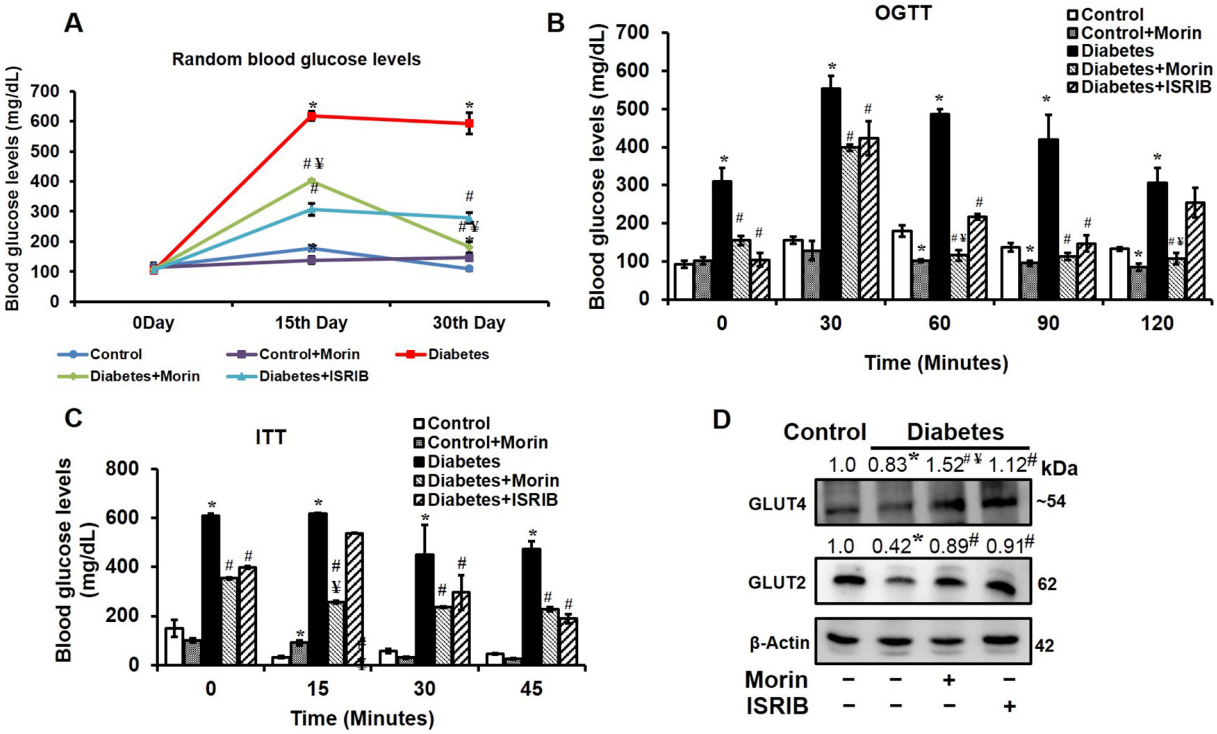

Fig. 3. Inhibition of ER stress improves glucose tolerance in diabetic rats. The graph represents (A) Random blood glucose levels (mg/dL) of the control and treated rats. (B) The bar graph indicates blood glucose levels (mg/dL) during Oral Glucose Tolerance Test (OGTT) in rats at different time points. (C) Insulin Tolerance Test (ITT) was performed on control and treated rats by measuring blood glucose levels at 15 min intervals. The graph represents mean blood glucose levels. (D) Immunoblots of GLUT4 and GLUT2 proteins in control and treated rat liver. β-Actin served as loading control. Data are expressed as mean ± SE. *p < 0.05 *vs* control, #p < 0.05 *vs* diabetic rats and ¥p < 0.05 *vs* ISRIB treated diabetic rats.

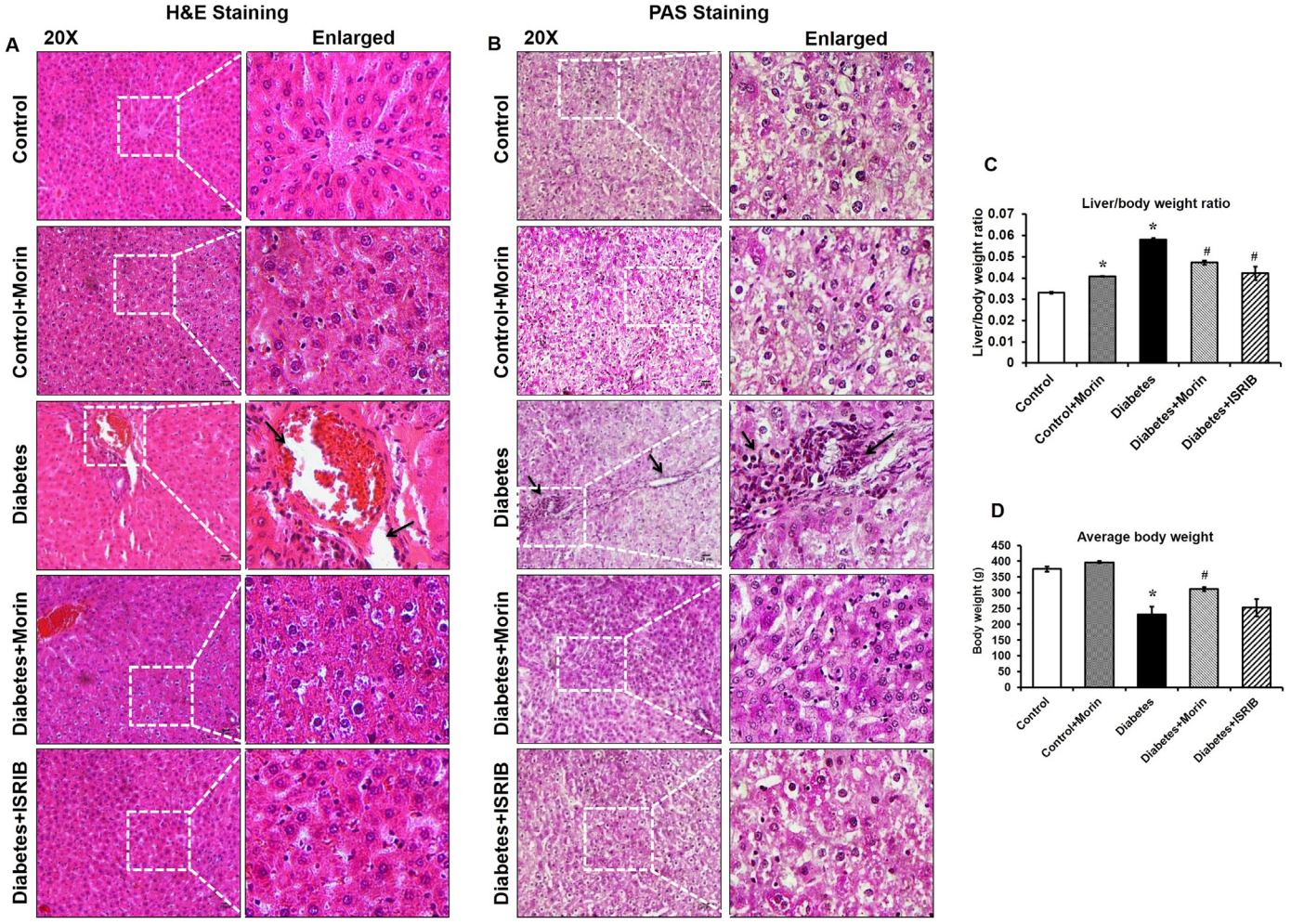

Fig. 4. ER stress inhibition averts liver toxicity during diabetes. (A) Images represent hematoxylin and eosin (H&E) staining on 5 μm liver tissue sections (magnification 20×, scale bar; 25 μm). Arrows in the enlarged images show the distortion and increased gapping between the sinusoids in diabetic rat liver. (B) Periodic acid-Schiff (PAS) staining of control and treated liver (magnification 20×, scale bar; 25 μm). Arrows indicate the lymphoid infiltration and formation of short septa in the diabetic rat liver. (C) Liver/body weight ratio of control and treated rats (D) Graph represents average body weight of the control and treated rats after four weeks of treatment. The bar graphs are presented as mean ± SE. *$p < 0.05$ *vs* control and #$p < 0.05$ *vs* diabetic rats.

(Fig. 4C, D).

We also inspected liver injury biomarkers in serum samples where diabetic rats showed significant ($p < 0.05$) increase in ALT (2.22 fold), AST (1.13 fold), ALP (2.17 fold) and total bilirubin levels (3.45 fold) compared to control (Fig. 5A–D). The enhancement in liver injury markers clearly demonstrate that hyperglycemia provoked liver damage. Importantly, ISRIB treatment efficiently reduced liver enzymes at par with control except for AST, depicting the critical role of ER stress in subduing liver functions (Fig. 5A–D). On a similar note, Morin remarkably reduced serum levels of hepatotoxicity markers confirming its anti-hepatotoxic potential.

Further, the expression of pro-inflammatory markers including CD36, nitrotyrosine, ICAM-1 and TNF-α were elevated significantly ($p < 0.05$) in the serum samples of diabetic rats (Fig. 5E). It was notable that, ISRIB and Morin treatment significantly ($p < 0.05$) subsided inflammation in the liver of diabetic rats (Fig. 5E). Thus, data demonstrate that hyperglycemic ER stress plays an important role in the progression of liver toxicity and Morin averts the same.

3.5. Morin prevents hyperglycemia induced proteotoxicity in rats

The findings so far indicated that ISRIB and Morin were consistent in preventing hyperglycemia induced oxidative stress and metabolic perturbations. We next sought to identify if Morin has ER stress inhibitory potential. Hence, we assessed the potency of Morin in regulating PDI activity, an ER specific protein folding enzyme. Morin treated rats showed up-regulation in PDI activity (1.84 fold; $p < 0.05$) compared to diabetic rats (Fig. 6A). This up-regulation in PDI activity by Morin is possibly due to enhanced total thiol levels (1.44 fold; $p < 0.05$) and GSH/GSSG ratio (1.41 fold; $p < 0.05$) in ER lumen (microsomal fractions) providing the substrate for optimal PDI activity (Fig. 6B, C).

Furthermore, Morin significantly attenuated ER stress marker proteins including phospho-PERK, ATF6, IRE1 and XBP1 (X-box binding protein 1) compared to diabetic rats as observed through immunoblotting studies (Fig. 6D–F). Additionally, the ER chaperone protein BiP (binding immunoglobulin protein) and calpain1 were lowered by Morin compared to diabetic rats suggesting that Morin possesses ER stress inhibitory capacity (Fig. 6G).

Studies on the mRNA expression of spliced XBP1, complete XBP1 and BiP were performed through RT-PCR which confirmed a significant reduction in the transcription of activated XBP1 (spliced XBP1) and BiP genes upon Morin treatment compared to diabetic rats revealing ER stress inhibitory potential of Morin similar to ISRIB (Fig. 6H, I). Thus, deactivation of UPR sensors and elevation in chaperone proteins provided strong evidence for the suppression of ER stress by Morin during hyperglycemia.

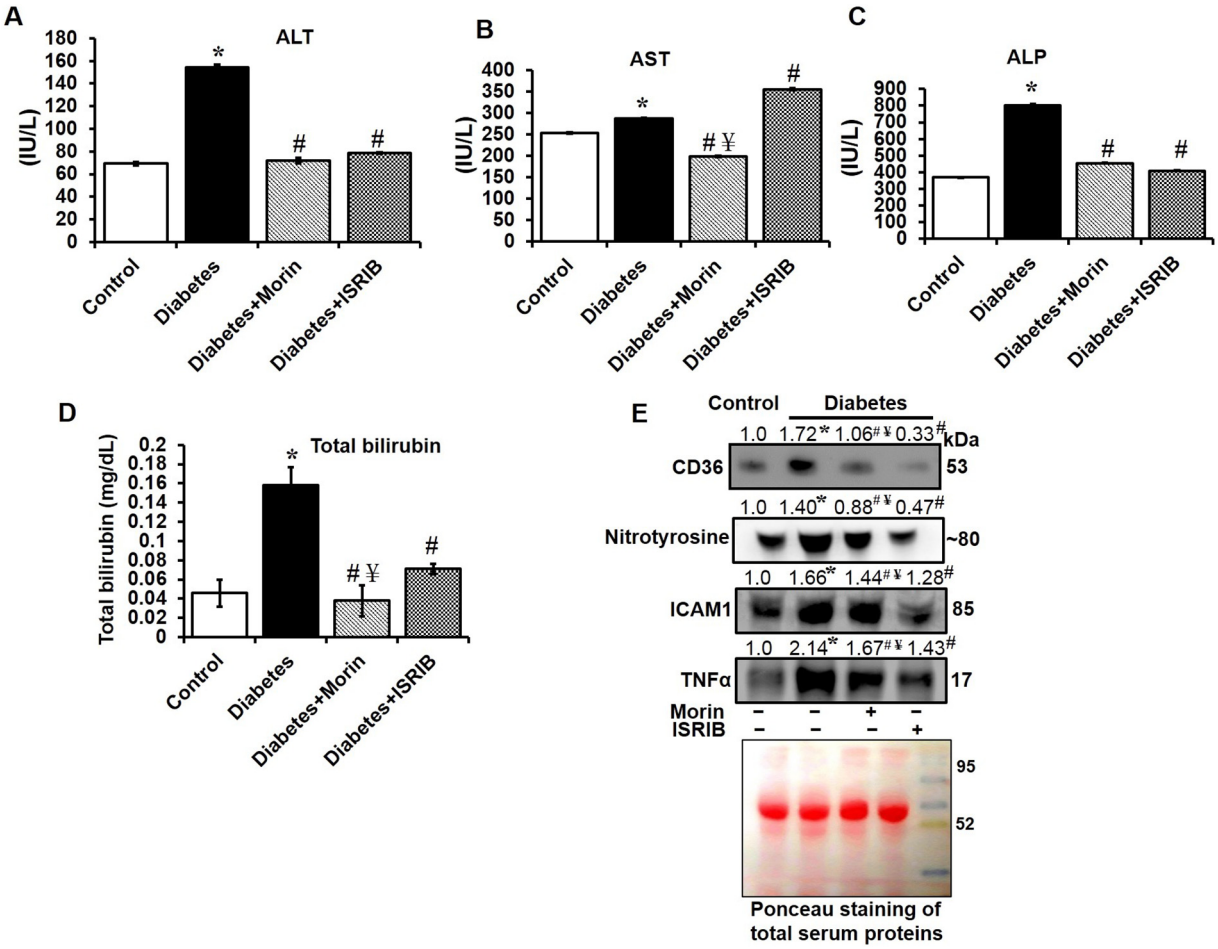

Fig. 5. ER stress inhibition lowers liver toxicity biomarkers and inflammation during diabetes. Liver function markers were determined in the serum samples of control and treated rats. Graph shows (A) alanine transaminase (ALT), (B) aspartate transaminase (AST), (C) alkaline phosphatase (ALP) and (D) total bilirubin levels. (E) Immunoblots of pro-inflammatory marker proteins: CD36, Nitrotyrosine, ICAM1, and TNFα were enhanced during diabetes which decreased with Morin and ISRIB treatment. Ponceau staining demonstrates equal loading of serum proteins. Biomarkers of liver toxicity data are expressed as mean ± SE. *p < 0.05 *vs* control, #p < 0.05 *vs* diabetic rats and ¥p < 0.05 *vs* ISRIB treated diabetic rats.

3.6. Morin intervenes with PERK-eIF2α-ATF4 axis to suppress hepatic cell death

Results exhibiting ER stress inhibitory capacity of Morin led us to further explore its intervention with the molecular pathway that prevents ER stress during diabetes. Data reveal that Morin directly interacts with PERK protein as evident by immunoblotting of samples obtained after pull down assay (Fig. 7A). Morin treatment further increased the interaction between BiP and PERK proteins compared to diabetic rats as observed by co-immunoprecipitation study (Fig. 7B). The enhanced interaction of BiP with PERK protein suggests that Morin down-regulates PERK activation in diabetic rats. Moreover, the down-regulation of the PERK pathway by Morin was evaluated through the assessment of its downstream targets *i.e.* eIF2α, ATF4 and CHOP proteins. Data showed that the expression of phospho-eIF2α, an immediate downstream molecular target of PERK, was significantly reduced (0.46 fold; $p < 0.05$), in Morin treated rats compared to diabetic group endorsing the ER stress modulatory effects of Morin *via* PERK signaling (Fig. 7C, D).

As PERK signaling executes its apoptotic response *via* ATF4/CHOP axis, we validated PERK response cascade by determining the protein expression of ATF4 and CHOP in treated liver tissues. Western blotting and immunohistochemistry data showed significant reduction in ATF4 and CHOP levels with Morin treatment compared to diabetic rats (Fig. 7E–I). Wide conviction states that CHOP directly inhibits Bcl2 to promote apoptosis. Thus, to confirm this, we examined the expression of anti-apoptotic protein Bcl2 and pro-apoptotic proteins including Bax, Bim and Caspase3 through immunoblotting. Bcl2 levels were down-regulated during hyperglycemia while Morin treatment prevented cell death as evident by upregulated Bcl2 levels (Fig. 7J). Prevention of apoptosis by Morin was further confirmed by the reduced expression of pro-apoptotic proteins including Bax, Bim and Caspase3 compared to diabetic rats (Fig. 7J, K). Similarly, ER stress inhibitor, ISRIB also lowered apoptosis induction in diabetic rats *via* inhibition of PERK-eIF2α-ATF4/CHOP axis (Fig. 7J, K). Additionally, expression of cleaved PARP protein was also reduced upon Morin treatment compared to diabetic group (Fig. 8A–C) depicting its potential in suppressing ER stress mediated DNA damage during T2D. Hyperglycemia induced proteotoxic apoptosis was further validated with increased nuclear translocation of AIF, Endonuclease G from mitochondria and concurrent cytosolic release of Cyt c compared to control. Nuclear translocation of AIF, Endo G and cytosolic release of Cyt c was significantly reduced by Morin treatment similar to that with ISRIB confirming attenuation of apoptosis (Fig. 8D–F).

Conclusively, the data explains a putative role of PERK-eIF2α-ATF4/CHOP axis in inducing hepatotoxic cell death during diabetes. The results strongly predict an ER stress inhibitory potential of Morin which prevented proteotoxic apoptosis *via* its novel molecular intervention with PERK-eIF2α-ATF4/CHOP pathway in diabetic rat liver.

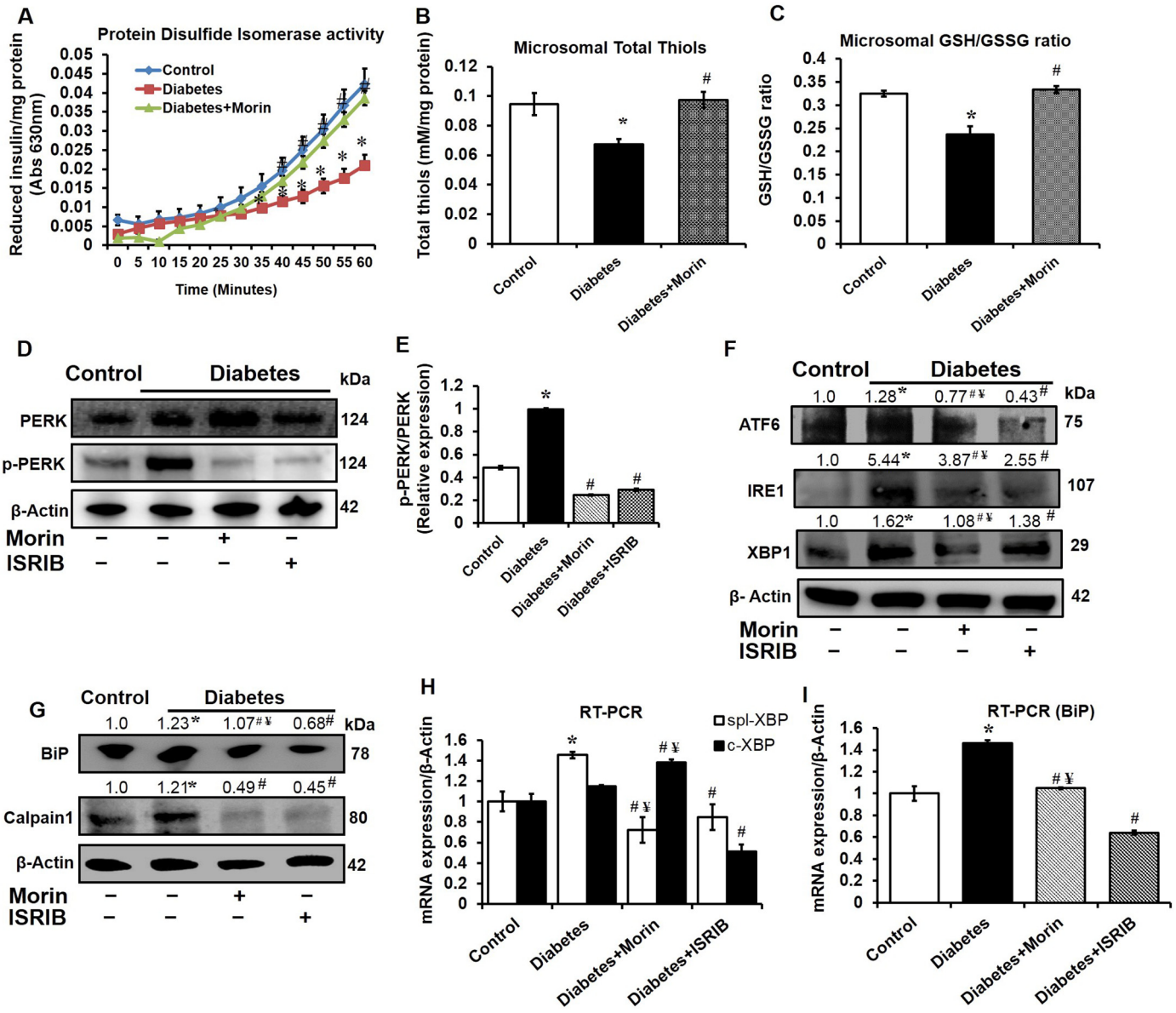

Fig. 6. Morin prevents high glucose induced ER stress in rat liver. (A) Protein disulfide isomerase (PDI) activity was assessed using the insulin reduction method. Data shows absorbance (630 nm) of reduced insulin/mg protein observed at regular intervals. (B) Microsomal total thiol levels, graph represents mM of total thiol/mg protein. (C) GSH/GSSG ratio was assessed in microsomal fractions of the liver. (D) Immunoblots of PERK and p-PERK, (E) the bar graph represents densitometric ratio of p-PERK/PERK. Immunoblots of (F) ATF6, IRE1, XBP1, (G) BiP and Calpain1 proteins in liver tissue lysate. mRNA expressions of (H) spliced-XBP1, complete-XBP1 and (I) BiP as determined through RT-PCR. Relative expression of mRNA was calculated by $2^{-\Delta\Delta ct}$ method. Data are expressed as mean ± SE. *p < 0.05 *vs* control, #p < 0.05 *vs* diabetic rats and ¥ p < 0.05 *vs* ISRIB treated diabetic rats.

4. Discussion

Literature reports in the recent past suggest a crucial role of ER stress in the progression of type 2 diabetes [7,8,11]. Oxidative stress has been found as a precipitating factor in disturbing the proteo-homeostasis in the cellular system. Liver, being the major site of glucose metabolism, becomes vulnerable to hyperglycemia induced oxidative toxicity. In this study, results demonstrate that hyperglycemia induced oxidative insult is interlinked with the proteotoxic (ER stress) cell death. The study also provides clear evidence of the putative involvement of oxidative stress with ER stress in regulating hepatotoxicity, glucose uptake and anti-oxidative enzyme activities in diabetic rats. Role of ER stress in causing liver damage was confirmed by its inhibition through ISRIB (chemical inhibitor) in streptozotocin/nicotinamide induced diabetic rats. ISRIB suppresses ER stress by dephosphorylating p-eIF2α at Ser51 residue to reconvert it into its activated form *i.e.* eIF2α which advances protein translation in the cells [36].

Furthermore, we investigated the ER stress inhibitory potential of Morin, a flavonol, for the first time and found that its interaction with the major UPR sensor, PERK, significantly prevented proteo-hepatotoxicity. Also, the anti-ER stress property of Morin was compared with the known chemical inhibitor of ER stress, ISRIB, to validate the efficacy of Morin in preventing ER stress mediated (proteotoxic) cell death. Morin is a phytochemical found in *Psidium guajava, Maclura tinctoria* and several other plants [20]. Previous reports from our lab demonstrated that Morin has a tremendous anti-oxidative potential to forestall drug induced reno- and hepato-toxicity [20,22–24]. The optimal dose of Morin that was selected for this study was based upon the results of a pilot study where 30 mg/Kg bwt./day showed enormous anti-oxidative and hepato-protective efficiency (Suppl. Figs. 1, 2). Herein, it was observed that Morin intervenes at the molecular level by directly interacting with PERK (Fig. 7A) which subsequently reduces the

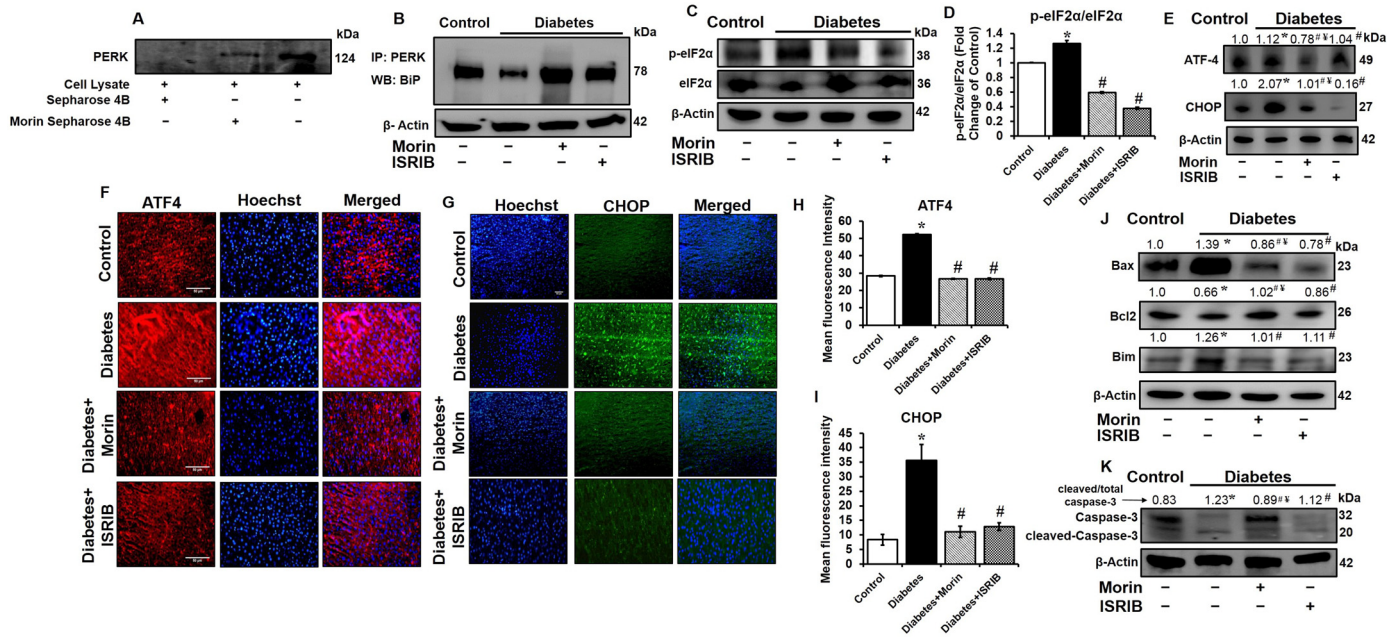

Fig. 7. Morin prevents hepatic ER stress mediated apoptosis by modulating PERK pathway. (A) Western blot of PERK demonstrating its interaction with Morin as observed through pull down assay. Proteins coupled with Morin were precipitated using activated CNBr-Sepharose beads followed by immunoblotting. (B) Co-immunoprecipitation study demonstrating the interaction of PERK with BiP, an ER specific chaperone. β-actin served as loading control (1/10th of the protein input). (C) Immunoblots of p-eIF2α and eIF2α proteins assessed in the total liver tissue sample. (D) The bar graph represents densitometric ratio of p-eIF2α/eIF2α. (E) Immunoblots of ATF-4 and CHOP proteins. Immunohistostaining of (F) ATF-4 and (G) CHOP protein on liver tissue section (magnification 20×, scale bar; 50 μm). The bar graphs show mean fluorescence intensity of (H) ATF-4 and (I) CHOP. (J) Western blots of Bax, Bcl2, Bim and (K) Caspase3 proteins. β-actin served as loading control for western blots. Data are expressed as mean ± SE. *p < 0.05 *vs* control, # p < 0.05 *vs* diabetic rats and ¥ p < 0.05 *vs* ISRIB treated diabetic rats.

phosphorylation of eIF2α, resulting in reduced expression of apoptotic transcription factors ATF4 and CHOP during ER stress (Fig. 7C–I). CHOP is reported to inhibit the expression of Bcl2, an anti-apoptotic protein which in turn, increases the activation of pro-apoptotic proteins [16,37] resulting in cell death. Similarly, we observed that the Bcl2 expression was increased in Morin treated diabetic rats (Fig. 7J) along with attenuated CHOP expression, supportive of the aforementioned reports.

Moreover, reports suggest that BiP chaperone masks the luminal domain of UPR sensor proteins and maintains them in their inactivated form under normal conditions [11]. Thus, the increased interaction of BiP with PERK protein validates the efficacy of Morin in deactivating the PERK signaling during diabetes (Fig. 7B). Importantly, our results indicate that Morin increases the reducing equivalents of ER lumen by increasing the total GSH and thiol levels which is necessary for the proper functioning of protein folding enzymes and chaperones. Enhanced PDI activity with Morin supported the conviction for its anti-proteotoxic potential which was significantly reduced during hyperglycemia (Fig. 6A–C). Additionally, Morin enhanced anti-oxidant enzymatic activities of catalase, thioredoxin reductase, glutathione S-transferase and glutathione peroxidase (Fig. 2D) and up-surged the expression of anti-oxidant proteins including SOD2, Nrf2, NQO1 and HO1 (Fig. 2F–H).

Impairment in the ER homeostasis is associated with aberrant calcium fluxes and calpain levels [38]. Lowered levels of calpain1 with Morin treatment indicates that it may modulate Ca^{2+} dependent proteolytic pathways. Previously, our lab reported that Morin interacts with the catalytic domains of PHLPP2 and Fyn kinase resulting into prevention of apoptotic cell death during acetaminophen induced liver toxicity [22]. Thus, the interaction of Morin with PERK and attenuation of its downstream signaling pathway (PERK-eIF2α-ATF4/CHOP axis) could be a plausible mechanism of the ER stress inhibitory capacity of Morin. Notably, Morin treatment prevented significant body weight loss of rats, increased glucose tolerance and reduced inflammation in diabetic rat liver which further adds to its strong anti-hyperglycemic, anti-hepatotoxic capacity along with the anti-ER stress potential. Findings of this study implicate that a) ER stress is one of the critical contributing factors in hyperglycemic hepatotoxicity and b) Morin is a potent candidate which suppresses ER stress mediated diabetic liver injury by inhibiting PERK signaling.

5. Conclusion

Our findings demonstrate for the first time that Morin possesses capacity to inhibit ER stress and also impacts glucose metabolism in liver. Morin exerts its protective effect by modulating the PERK-eIF2α pathway as evident through reduced expression of its downstream targets. Moreover, this study also explored the link between hyperglycemia induced ER-stress and oxidative insult during diabetes. The anti-ER stress and anti-hyperglycemic potential of Morin show possibilities of its being exploited as a bioactive supplement in managing ER stress during type 2 diabetes.

Supplementary data to this article can be found online at https://doi.org/10.1016/j.cellsig.2019.03.008.

Conflict of interest

The authors declare that they have no conflict of interest associated with this manuscript.

Funding

This work was supported by the Council of Scientific and Industrial Research (CSIR) - Network project grant (BSC 0106) to PK. VKP is thankful to the University Grants Commission (UGC), New Delhi, India. AM and MFK to Council of Scientific and Industrial Research (CSIR), New Delhi, India for their Senior Research Fellowships (SRF).

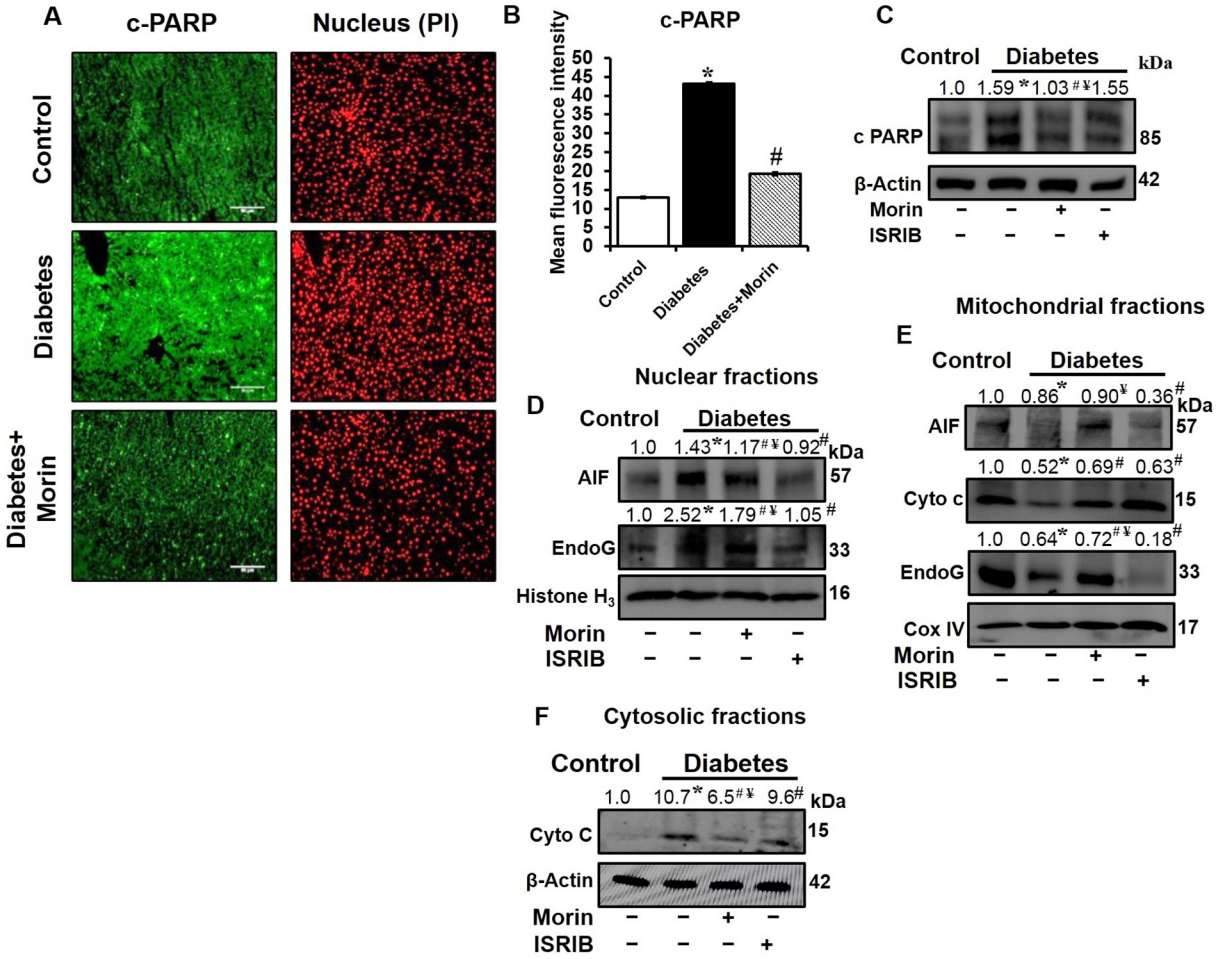

Fig. 8. Inhibition of ER stress by Morin prevents apoptotic cell death. (A) Expression of DNA damage marker protein, PARP, was observed through immunohistostaining of cleaved PARP (c-PARP) on 5 μm liver tissue sections (magnification 20×, scale bar; 50 μm). (B) The bar graph represents mean fluorescence intensity of c-PARP. (C) Western blot of cleaved-PARP measured in total liver lysates. Immunoblots of (D) AIF and EndoG in nuclear fractions of control and treated rats. Histone (H3) served as nuclear loading control. (E) Western blots of AIF, Cytochrome c and EndoG in the mitochondrial fraction. CoxIV served as mitochondrial protein loading control. (F) Cytosolic level of Cytochrome c protein. β-actin served as the loading control for cytosolic fractions. Data are expressed as mean ± SE. *p < 0.05 *vs* control. # p < 0.05 *vs* diabetic rats and ¥ p < 0.05 *vs* ISRIB treated diabetic rats.

Author contributions

VKP and PK conceptualized and designed the study. VKP, AM and MFK performed the experiments. VKP and AM analyzed and interpreted the data. VKP and PK wrote the manuscript. All authors approved the final version of the manuscript.

Acknowledgment

Authors are thankful to the Institutional Manuscript Review Committee of CSIR-IITR for reviewing the manuscript and allocating the manuscript number 3507.

References

[1] J. Wang, J. Tan, J. Luo, et al., Enhancement of scutellarin oral delivery efficacy by vitamin B12-modified amphiphilic chitosan derivatives to treat type II diabetes induced-retinopathy, J. Nanobiotechnol. 15 (2017) 18, https://doi.org/10.1186/s12951-017-0251-z.

[2] S. Dronavalli, I. Duka, G.L. Bakris, The pathogenesis of diabetic nephropathy, Nat. Clin. Pract. Endocrinol. Metab. 4 (2008) 444–452, https://doi.org/10.1038/ncpendmet0894.

[3] P. Bharadwaj, N. Wijesekara, M. Liyanapathirana, et al., The link between type 2 diabetes and neurodegeneration: roles for amyloid-β, amylin, and tau proteins, J. Alzheimers Dis. 59 (2017) 421–432, https://doi.org/10.3233/JAD-161192.

[4] X. Hu, T. Bai, Z. Xu, Q. Liu, Y. Zheng, L. Cai, Pathophysiological fundamentals of diabetic cardiomyopathy, Compr. Physiol. 7 (2017) 693–711, https://doi.org/10.1002/cphy.c160021.

[5] M.M. Adeva-Andany, N. Pérez-Felpete, C. Fernández-Fernández, C. Donapetry-García, C. Pazos-García, Liver glucose metabolism in humans, Biosci. Rep. 36 (2016) e00416, , https://doi.org/10.1042/BSR20160385.

[6] M. Torbenson, Y.Y. Chen, E. Brunt, O.W. Cummings, M. Gottfried, S. Jakate, Y.C. Liu, M.M. Yeh, L. Ferrell, Glycogenic hepatopathy: an under recognized hepatic complication of diabetes mellitus, Am. J. Surg. Pathol. 30 (2006) 508–513.

[7] L. Salvado, X. Palomer, E. Barroso, M. Vázquez-Carrera, Targeting endoplasmic reticulum stress in insulin resistance, Trends Endocrinol. Metabol. 26 (2015) 438–448.

[8] V.K. Pandey, A. Mathur, P. Kakkar, Emerging role of Unfolded Protein Response (UPR) mediated proteotoxic apoptosis in diabetes, Life Sci. 216 (2018) 246–258.

[9] M.J. Davies, Protein oxidation and peroxidation, Biochem. J. 473 (2016) 805–825, https://doi.org/10.1042/BJ20151227.

[10] A.A. Ramanathan, A. Mehta, C.M. Artlett, The impact of the unfolded protein response and the Hexosamine biosynthetic pathway on glycosylation, Glycobiol. Insights (2017) 1–12, https://doi.org/10.1177/1179251516688214.

[11] R. Cunard, Endoplasmic reticulum stress in the diabetic kidney, the good, the bad and the ugly, J. Clin. Med. 4 (2015) 715–740, https://doi.org/10.1152/ajprenal.00021.2011.

[12] C. Piperi, C. Adamopoulos, A.G. Papavassiliou, XBP1: a pivotal transcriptional regulator of glucose and lipid metabolism, Trends Endocrinol. Metab. 27 (2016) 119–122, https://doi.org/10.1016/j.tem.2016.01.001.

[13] F. Urano, X.Z. Wang, A. Bertolotti, et al., Coupling of stress in the ER to activation of JNK protein kinases by transmembrane protein kinase IRE1, Science 287 (2000) 664–666, https://doi.org/10.1126/science.287.5453.664.

[14] L. Dong, L. Xing, Z. Ti, et al., IRE1–RACK1 axis orchestrates ER stress preconditioning-elicited cytoprotection from ischemia/reperfusion injury in liver, J. Mol. Cell Biol. 8 (2016) 144–156.

[15] R. Liu-Bryan, R. Terkeltaub, Emerging regulators of the inflammatory process in osteoarthritis, Nat. Rev. Rheumatol. 11 (2015) 35–44, https://doi.org/10.1038/

nrrheum.2014.162.
[16] H. Muaddi, M. Majumder, P. Peidis, et al., Phosphorylation of eIF2α at serine 51 is an important determinant of cell survival and adaptation to glucose deficiency, Mol. Biol. Cell 21 (2010) 3220–3231, https://doi.org/10.1091/mbc.E10-01-0023.
[17] T.D. Baird, L.R. Palam, M.E. Fusakio, et al., Selective mRNA translation during eIF2 phosphorylation induces expression of IBTKα, Mol. Biol. Cell 25 (2014) 1686–1697, https://doi.org/10.1091/mbc.E14-02-0704.
[18] W. B'chir, A.C. Maurin, V. Carraro, et al., The eIF2α/ATF4 pathway is essential for stress-induced autophagy gene expression, Nucleic Acids Res. 41 (2013) 7683–7699, https://doi.org/10.1093/nar/gkt563.
[19] W. B'chir, C. Chaveroux, V. Carraro, et al., Dual role for CHOP in the crosstalk between autophagy and apoptosis to determine cell fate in response to amino acid deprivation, Cell. Signal. 26 (2014) 1385–1391, https://doi.org/10.1016/j.cellsig.2014.03.009.
[20] R. Kapoor, P. Kakkar, Protective role of morin, a flavonoid, against high glucose induced oxidative stress mediated apoptosis in primary rat hepatocytes, PLoS One 7 (2012) e41663, , https://doi.org/10.1371/journal.pone.0041663.
[21] P. Paoli, P. Cirri, A. Caselli, et al., The insulin-mimetic effect of Morin: a promising molecule in diabetes treatment, Biochim. Biophys. Acta 1830 (2013) 3102–3111, https://doi.org/10.1016/j.bbagen.2013.01.017.
[22] F. Rizvi, A. Mathur, S. Krishna, M.I. Siddiqi, P. Kakkar, Suppression in PHLPP2 induction by morin promotes Nrf2-regulated cellular defenses against oxidative injury to primary rat hepatocytes, Redox Biol. 6 (2015) 587–598, https://doi.org/10.1016/j.redox.2015.10.002.
[23] F. Rizvi, A. Mathur, P. Kakkar, Morin mitigates acetaminophen-induced liver injury by potentiating Nrf2 regulated survival mechanism through molecular intervention in PHLPP2-Akt-Gsk3β axis, Apoptosis 20 (2015) 1296, https://doi.org/10.1007/s10495-015-1160-y.
[24] A. Mathur, F. Rizvi, P. Kakkar, PHLPP2 down regulation influences nuclear Nrf2 stability via Akt-1/Gsk3β/Fyn kinase axis in acetaminophen induced oxidative renal toxicity: protection accorded by morin, Food Chem. Toxicol. 89 (2016) 19–31, https://doi.org/10.1016/j.fct.2016.01.001.
[25] R. Kapoor, S. Srivastava, P. Kakkar, Bacopa monnieri modulates antioxidant responses in brain and kidney of diabetic rats, Environ. Toxicol. Pharmacol. 27 (2009) 62–69, https://doi.org/10.1016/j.etap.2008.08.007.
[26] T. Szkudelski, Streptozotocin–nicotinamide-induced diabetes in the rat. Characteristics of the experimental model, Exp. Biol. Med. 237 (2012) 481–490.
[27] A. Ghasemi, S. Khalifi, S. Jedi, Streptozotocin-nicotinamide-induced rat model of type 2 diabetes, Acta Physiol. Hung. 101 (2014) 408–420.
[28] N. Kubota, K. Tobe, Y. Terauchi, et al., Disruption of insulin receptor substrate 2 causes type 2 diabetes because of liver insulin resistance and lack of compensatory beta-cell hyperplasia, Diabetes 49 (2000) 1880–1889.
[29] S. Andrikopoulos, A.R. Blair, N. Deluca, et al., Evaluating the glucose tolerance test in mice, Am. J. Physiol. Endocrinol. Metab. 295 (2008) E1323–E1332.
[30] M.M. Watanabe, F.R.M. Laurindo, D.C. Fernandes, Methods of measuring protein disulfide isomerase activity: a critical overview, Front Chem. 2 (2014) 73.
[31] D.M. Townsend, Y. Manevich, L. He, et al., Nitrosative stress–induced S-glutathionylation of protein disulfide isomerase leads to activation of the unfolded protein response, Cancer Res. 69 (2009) 7626–7634, https://doi.org/10.1158/0008-5472.CAN-09-0493.
[32] P. Bernardoni, B. Fazi, A. Costanzi, et al., Reticulon1-C modulates protein disulphide isomerase function, Cell Death Dis. 4 (2013) e581, , https://doi.org/10.1038/cddis.2013.113.
[33] I. Dimauro, T. Pearson, D. Caporossi, M.J. Jackson, A simple protocol for the subcellular fractionation of skeletal muscle cells and tissue, BMC Res. Notes 5 (2012) 513, https://doi.org/10.1186/1756-0500-5-513.
[34] B. Cox, A. Emili, Tissue subcellular fractionation and protein extraction for use in mass-spectrometry-based proteomics, Nat. Protocol. 1 (2006) 1872–1878, https://doi.org/10.1038/nprot.2006.273.
[35] G.S. Cottrell, B. Padilla, S. Pikios, et al., Ubiquitin dependent down-regulation of the neurokinin-1 receptor, J. Biol. Chem. 281 (2006) 27773–27783, https://doi.org/10.1074/jbc.M603369200.
[36] C. Sidrauski, A.M. McGeachy, N.T. Ingolia, P. Walter, The small molecule ISRIB reverses the effects of eIF2α phosphorylation ontranslation and stress granule assembly, elife 4 (2015) e05033, , https://doi.org/10.7554/eLife.05033.
[37] I. Tabas, D. Ron, Integrating the mechanisms of apoptosis induced by endoplasmic reticulum stress, Nat. Cell Biol. 13 (2011) 184–190.
[38] D. Zheng, G. Wang, S. Li, et al., Calpain-1 induces endoplasmic reticulum stress in promoting cardiomyocyte apoptosis following hypoxia/reoxygenation, Biochim. Biophys. Acta 5 (2015) 882–892.